International Journal of Applied Engineering Research
ISSN 0973-4562 Volume 7, Number 12 (2012) pp. 1391-1405

https://dx.doi.org/10.37622/IJAER/7.12.2012.1391-1405

Investigation of the Penetration Capability of an Axi-Symmetric Cross Jet in a Turbulent Fluid Flow through a Circular Pipe

Snehamoy Majumder[1], Debajit Saha[2] and Pritam Das[3]

[1]Associate Professor & Corresponding Author, Dept. of Mechanical Engineering, Jadavpur University, Kolkata-700 032, West Bengal, India,

[2]Research Scholar, Dept. of Mechanical Engineering, Jadavpur University, Kolkata,

[3]Research Scholar, Dept. of Mechanical Engineering, Jadavpur University, Kolkata,

Abstract

The side mass injection flow in a main turbulent fluid flow through a circular duct is very important since it is encountered in many industrial appliances like the Gas Turbine Combustion chamber, different cooling systems etc. In the present study, a numerical analysis of the turbulent fluid flow through a circular duct with side wall mass injection, both having axial symmetry, have been carried out using modified $\kappa-\varepsilon$ model, considering streamline curvature effects. The different conditions of flow which provide optimum mixing and penetration of the side jet with the main flow were determined from the computational results. The effects of ratio of the side injection velocity to the inlet mean velocity, axial location and extent of the side injection site on the penetration depth of the side injected flow, strength and size of the recirculation bubble and the mixing of two mutually cross turbulent jets have been studied in details. The principle observation from the numerical analysis was that the effects of side mass injection are very important on the main bulk flow and it has a vital role in the formation of recirculation bubble in the duct. Efforts have been given to study the optimum axial position of the side injection site for the best possible penetration and mixing. The velocity distributions of different parameters and vector plotting of the absolute velocity along with the stream line plotting visualizing the details flow field have been done thoroughly.

Keywords: Turbulent Flow, Side Wall Mass Injection, Streamline Curvature, Penetration, Recirculation Bubble, Velocity Ratio.

1 Introduction

Turbulent fluid flows in non-inertial frame of reference are encountered in a variety of engineering applications. An important property of turbulence lies in its ability to transport and mix fluid much more effectively than a comparable laminar flow. The phenomena of side injection flow injected normally or at an angle into a main turbulent bulk flow occur in various industrial processes. In a gas turbine combustor, generally, the placements, size and injection velocities of fluid greatly affect the performance of the combustor. Earlier studies of turbulent flow include the experimental investigation on the fully developed turbulent flow by Laufer [1]. Barcilon and Curtet [2] experimentally found that the Craya-Curtet number is an important parameter for characterizing the re-circulation zones that are often associated with mixing of jets. The numerical investigation of destabilization of the flow in a cylindrical duct has been reported by using the modification of standard model for streamline curvature by Launder and Spalding [5]. Ei-Nashar [4] investigated turbulent flow in an annulus with injection at the inner tube. Their observation concludes that injection caused a pronounced decrease in the mean axial velocities near the porous tube and a shift of the position of maximum velocity towards the outer tube. The $\kappa - \varepsilon$ turbulence model was adopted by Chang and Chen [8] for the numerical investigation for the mixing of oppositely heated line jets discharged normally or at an angle into a horizontal cold cross flow in a rectangular channel. The results showed that there was a strong recirculation near the downstream region of the nozzle opening. Turbulent flow fields resulting from an oblique jet injecting from a rectangular side inlet duct into a rectangular main duct with an aspect ratio 3.75 without a forced cross flow were presented by Tong-Miin *et al.* [9]. Their investigation showed that with increase in injection angle the size of the recirculation zone generated immediately behind the downstream edge increases. The resultant flow structure generated by the interaction of the suction into a circular duct and a cross flow was studied by Hold *et al.* [10]. Tao *et al.* [11] numerically investigated the effects of a row of jets discharging normally into a confined cylindrical cross flow using the control volume based finite difference method. Kelmen *et al.* [12] have examined the mixing of sub-millimeter diameter jets issuing into a turbulent cross flow with a combination of laser diagnostic techniques. A range of cross jet momentum ratios, cross flow temperature and turbulence intensities were investigated to examine the influence on the jet mixing. Ting-ting and Shao-hua [14] investigated interaction of turbulent jets with lateral injection into a cross flow. The results showed that the injection angle and jet to cross flow velocity ratio can change the flow fields and this change is comparatively high in the upstream side. The effects of side inlet angle on fuel air mixing phenomena in three dimensional side dump combustor with dual opposite curved side inlet ducts were numerically investigated by Ko [13]. The formation of re-circulation zone in low Re number turbulence was investigated by Kollman and Umont [17]. It was concluded that axi-symmetric flow generates a re-circulation bubble by a closed stream surface. The work on compressible tangentially injected swirling flow in the nozzle of air-jet spinning by Guo *et al.* [16] showed that with increase in the injection angle or injector diameter or injector number the velocity in the downstream of the injector will increase and the location of the vortex

breakdown shifts to the downward side.

The present work pertains to the numerical investigation of the penetration of the side mass injection into the main turbulent flow through a circular duct as well as how the strength and size of the recirculation bubble changes with the ratio of injection velocity to the mean inlet velocity. Also, this study focused to estimate the position of the side mass injection for which the recirculation will be present or not. Standard $k-\varepsilon$ model together with modification due to streamline curvature has been employed to resolve the re-circulating flow regions accurately. The flow has been considered to be steady, incompressible, turbulent, non-reacting and axi-symmetric. The control volume formulation with power law scheme of S. V. Patankar [6] with SIMPLER algorithm has been adopted. The momentum and the $k-\varepsilon$ equations have been solved with the aid of wall function. It has been observed that the onset of recirculation as well as length and breadth of the recirculation bubble strongly depends on the side injection.

2 Geometrical Description and Mathematical Model

The geometry of the flow is shown in fig.1. Figure 1 shows the essential features of the cylindrical axi-symmetric turbulent fluid flow, which has been considered in the present study with entries in the duct from both radial and axial directions. The cylindrical coordinate $r-x$ has been considered. Since the flow is axi-symmetric, so only the axis to the wall i.e., half of the circular duct has been considered for the numerical computation as shown in the figure 1. The inlet velocity is shown as U_{in} and the radially inward velocity of side injection as V_{inj}. The axial extent of side injection is from X_1 to X_2, while the diameter of the duct is given by D. Here, the angle of side injection is 90°. Keeping this geometrical configuration the numerical investigation of turbulent fluid flow have been done by varying the inlet flow velocity, side injection velocity, the extent and axial position of side injection.

For the present investigation the axial length of the duct is considered as L = 9 m, the diameter of the duct, D = 0.1534 m, Air density, ρ =1.235 kg/m^3, Molecular viscosity of air, μ_l =1.853×10^{-5} kgm^{-1}s^{-1}. The Reynolds number is defined as $R_e = (\rho U_{mean} D)/\mu_l$, where U_{mean} is the mass-averaged axial inlet velocity. The Reynolds number R_e varies from 2045 to 10,224.

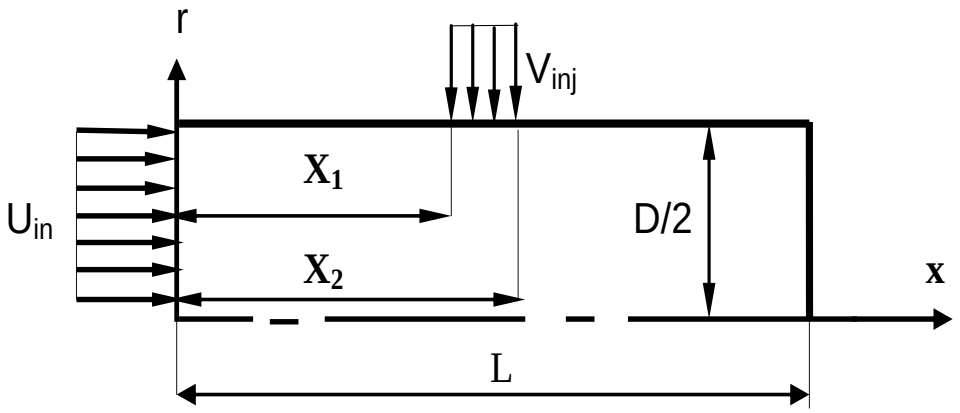

Figure 1, Schematic diagram of the axi-symmetric circular duct with main turbulent flow and normal side injection.

3 Governing Equations

The mass and momentum conservation equations in axi-symmetric cylindrical co-ordinate system for the turbulent mean flow with eddy viscosity model is given as follows:

Continuity Equation:

$$\frac{\partial(\rho\bar{u})}{\partial x}+\frac{\mathbf{1}}{r}\frac{\partial(\rho r\bar{v})}{\partial r}=\mathbf{0} \tag{1}$$

Momentum Equations:

Axial Component (x-component):

$$\rho\left[\bar{v}\frac{\partial\bar{u}}{\partial r}+\bar{u}\frac{\partial\bar{u}}{\partial x}\right]=-\frac{\partial\bar{p}}{\partial x}+\frac{\partial}{\partial x}\left(\mu_{eff}\frac{\partial\bar{u}}{\partial x}\right)+\frac{1}{r}\frac{\partial}{\partial r}\left(r\mu_{eff}\frac{\partial\bar{u}}{\partial r}\right)+\left[\frac{\partial}{\partial x}\left(\mu_{eff}\frac{\partial\bar{u}}{\partial x}\right)+\frac{1}{r}\frac{\partial}{\partial r}\left(r\mu_{eff}\frac{\partial\bar{v}}{\partial x}\right)\right] \tag{2}$$

Radial Component (r-component):

$$\rho\left[\bar{v}\frac{\partial\bar{v}}{\partial r}+\bar{u}\frac{\partial\bar{v}}{\partial x}\right]=-\frac{\partial\bar{p}}{\partial r}+\frac{\partial}{\partial x}\left(\mu_{eff}\frac{\partial\bar{v}}{\partial x}\right)+\frac{1}{r}\frac{\partial}{\partial r}\left(r\mu_{eff}\frac{\partial\bar{v}}{\partial r}\right)+\left[\frac{\partial}{\partial x}\left(\mu_{eff}\frac{\partial\bar{u}}{\partial r}\right)+\frac{1}{r}\frac{\partial}{\partial r}\left(r\mu_{eff}\frac{\partial\bar{v}}{\partial r}\right)\right]-2\mu_{eff}\frac{\bar{v}}{r^2} \tag{3}$$

Where, $\bar{u}$ and $\bar{v}$ the mean velocity components along x and r directions respectively.

The effective viscosity is,

$$\mu_{eff}=\mu_l+\mu_t \tag{4}$$

Where, μ_l and μ_t are molecular or laminar viscosity and eddy or turbulent viscosity respectively. The eddy viscosity is given by,

$\mu_t = \rho C_\mu \kappa^2 / \varepsilon$

where, C_μ is an empirical coefficient.

The modified form of the empirical constant C_μ is given as,

$$C_\mu = \frac{-K_1 K_2}{\left[1 + 8K_1^2 \frac{k^2}{\varepsilon^2}\left(\frac{\partial U_S}{\partial n} + \frac{U_S}{R_C}\right)\frac{U_S}{R_c}\right]} \tag{5}$$

Here, $U_S = \sqrt{\bar{u}^2 + \bar{v}^2}$

R_c is the radius of curvature of the concerned streamline ($\psi = $constant). To capture the streamline curvature effects the modifications has been incorporated according to Rodi and Leschziner [7] and Majumder and Sanyal [15]. These have been found effective to provide realistic solutions in the conditions of severe streamline curvature.

The $k-\varepsilon$ equations are given by,

$k-$Equation:

$$\rho\left[\bar{u}\frac{\partial k}{\partial x} + \bar{v}\frac{\partial k}{\partial r}\right] = \frac{\partial}{\partial x}\left[\left(\mu_l + \frac{\mu_t}{\sigma_k}\right)\frac{\partial k}{\partial x}\right] + \frac{1}{r}\frac{\partial}{\partial r}\left[r\left(\mu_l + \frac{\mu_t}{\sigma_k}\right)\frac{\partial k}{\partial r}\right] + \rho G - \rho\varepsilon \tag{6}$$

Where, G is the production term and given by:

$$G = \mu_t\left[2\left\{\left(\frac{\partial \bar{v}}{\partial r}\right)^2 + \left(\frac{\partial \bar{u}}{\partial x}\right)^2 + \left(\frac{\bar{v}}{r}\right)^2\right\} + \left(\frac{\partial \bar{u}}{\partial r} + \frac{\partial \bar{v}}{\partial x}\right)^2\right]$$

$\varepsilon-$Equation:

$$\rho\left[\bar{u}\frac{\partial \varepsilon}{\partial x} + \bar{v}\frac{\partial \varepsilon}{\partial r}\right] = \frac{\partial}{\partial x}\left[\left(\mu_l + \frac{\mu_t}{\sigma_\varepsilon}\right)\frac{\partial \varepsilon}{\partial x}\right] + \frac{1}{r}\frac{\partial}{\partial r}\left[r\left(\mu_l + \frac{\mu_t}{\sigma_\varepsilon}\right)\frac{\partial \varepsilon}{\partial r}\right] + C_{\varepsilon 1} G\frac{\varepsilon}{k} - C_{\varepsilon 2}\frac{\varepsilon^2}{k} \tag{7}$$

Here, $C_{\varepsilon 1}, C_{\varepsilon 2}, \sigma_k$ and σ_ε are the empirical turbulence constants, and some typical values of these constants in the standard $\kappa-\varepsilon$ model are recommended by Launder and Spalding which are given as follows, $C_{\varepsilon 1}$ = 1.44, σ_k = 1.0, $C_{\varepsilon 2}$ = 1.92

and σ_{ε} = 1.3. The standard wall function has been adopted from Launder and Spalding (1974) for the solution of the $k-\varepsilon$ equations for the problem investigated here.

3 Results and Discussions

The control volume formulation of Patankar [6] with SIMPLER algorithm and power-law scheme has been employed for the computational analysis. Detailed study of the effect of side injection on the main turbulent flow with axial inlet has been carried out after establishing that the turbulence-modeling scheme adopted for the study to be quite appropriate. Two arrays of 201 X 101 and 501 X 201 grid points in axial and radial directions, respectively, have been used. It has been observed that the grid independent study has shown 0.001% change in the stream wise velocity change. The grid array of 201 X 101 has been used for all subsequent results reported here.

3.1 Validation of the Present Results with Benchmark Solutions

The present results have been validated with the benchmark solution [3]. Figure 2 presents the validation for the turbulent model used in the present analysis using the experimental results of Olson and Eckert [3] for a turbulent flow in a porous circular tube with uniform fluid injection throughout the tube wall. In fig. 2 the friction factor computed from the experimental results of Olson and Eckert have been compared with the friction factor obtained from the numerical analysis. Good agreement between the experimental results and numerical prediction establishes the validity of the numerical method used in the present study for the turbulent fluid flow through a circular duct with side mass injection.

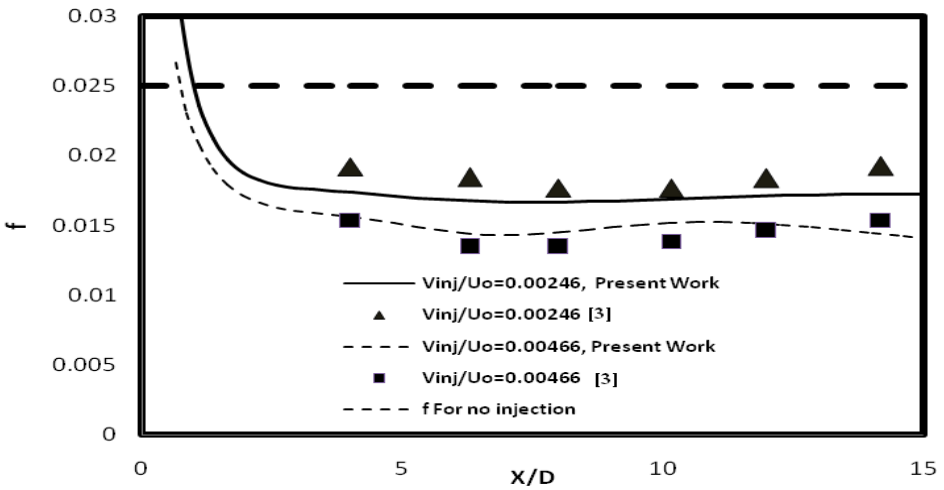

Figure 2, Validation of the present numerical method.

3.2 Effects of Axial Velocity on Side Mass Injection

In fig. 3, velocity vector and flooded streamline contour for side injection without main flow i.e., $U_{in} = 0$ has been shown. From the figure, we can see that the flow coming vertically from the side wall bifurcates and turns into two oppositely rotating vortices. This is physically possible and this finding is amply supported by the diagram. Here the flow penetrates up to the axis of the duct.

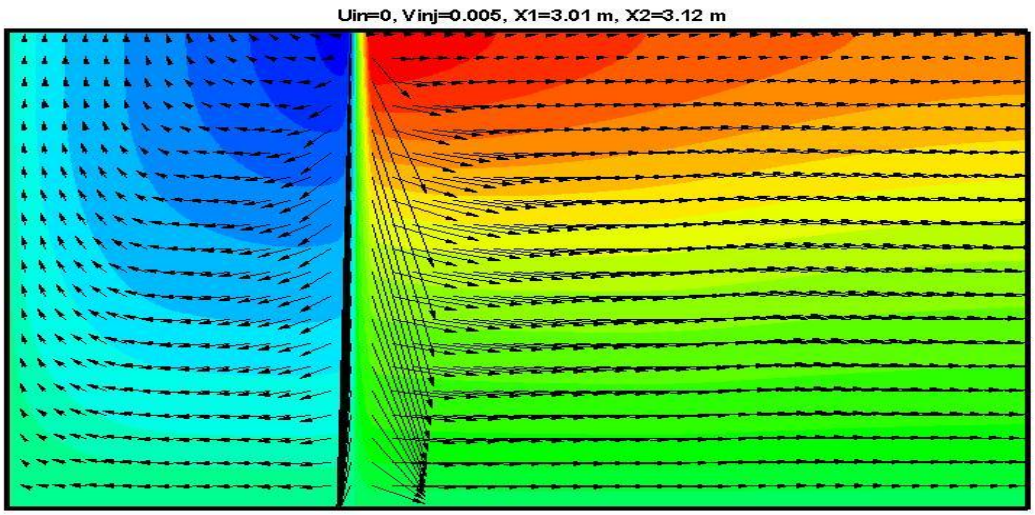

Figure 3, Vector plotting and flooded stream line contour for side injection without main flow.

Figure 4 shows the effect of side mass injection on the main bulk turbulent flow with the variation of the axial velocity. Figure 4 is a streamline contour plot along with velocity vector diagram. The side injection velocity is taken as V_{inj} = -0.05 m/s and the inlet axial velocity has been varied from 0.5 m/s to 3 m/s. From the figure it is evident that the side mass injection penetrates deep into the main bulk fluid mass and the penetration depth is quite considerable as expected from the physical condition of the flow. With an increase of the inlet axial velocity keeping the side injection velocity constant the penetration effect reduces i.e. the penetration depth gradually decreases with a gradual increase of inlet velocity. This is physically possible due to the fact that the momentum of the inlet main axial flow is increased due to the increase in axial velocity which forces the side injection flow not to penetrate further into the main flow. Thus the rapid mixing of the two cross flow has been observed to reduce by increasing the inlet velocity of the main flow. It definitely affects the flow pattern of the upstream side fluid motion in the cylindrical duct, since under such conditions the Entrance length usually increases.

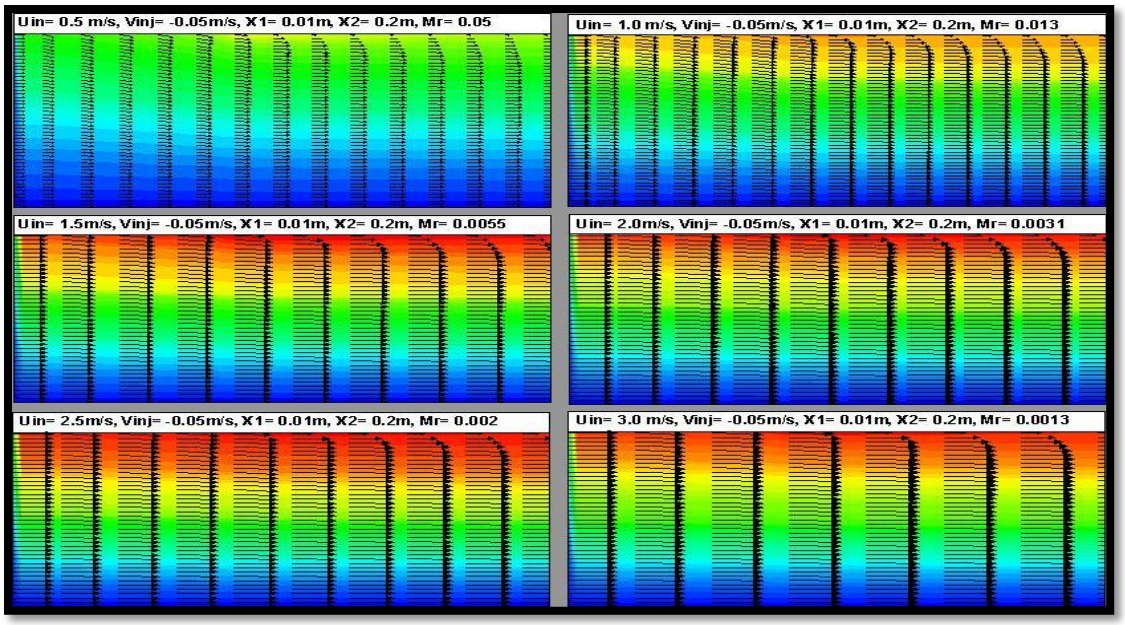

Figure 4, Effects of the axial velocity on the side mass injection penetration.

3.3 Effect of Side Injection Velocity

Figure 5 shows the streamline contours, colored flood contours and vector diagrams with inlet uniform axial velocity U_{in} = 0.5 m/s and side injection velocity, V_{inj} =-0.5 m/s to -3 m/s located at $X_1 = 0.01$ to $X_2 = 0.2$. It is observed from the figure that with the increase of the side injection velocity the side jet penetration increases. With the increase of the side injection velocity it was observed that secondary flow or recirculation bubble appears. The main flow and side injection flow directions are mutually orthogonal to each other and there is a resistance offered by the side injection mass to the main flow. Consequently there is a drop in pressure in the upstream side of the flow terminating into a low velocity flow reversal zone. The ultimate consequence is the generation of a recirculatory flow. The length and breadth of recirculation bubble increases with the increase in the side injection velocity. This is also signifying that the more is the side injection velocity, the more will be the penetrating capability of the circular jet through the main flow, which is flowing with a constant velocity. In the combustion chamber the flames occasionally wipe out at high fluid velocity. This recirculation is very important for the combustion flame sustenance and stability as it provides a residence for the flame. The velocity of the fluid at the vicinity of the recirculation zone is low and the combustion flame resides here for longer time providing it enough opportunity for complete combustion of the fuels. It is also evident that as the size of recirculation becomes larger it strongly influences the flow. The recirculatory flow by enveloping the low pressure zone reduces the space for the air flow passing through the duct and affects the upstream flow. The main bulk fluid flow is moving in a tortuous fashion imparting a screwing motion which entrains the adjacent fluid causing the recirculatory secondary flows as shown in the vector plotting. There are some adverse effects which arise due to the

presence of the recirculation bubble. Since the residence time is increased for the combustion flame, therefore there are probabilities of accumulation of NOx and temperature rise occurs locally at this region. These may be unwanted for the applications where cooling is important and NOx generation and accumulation has adverse effects.

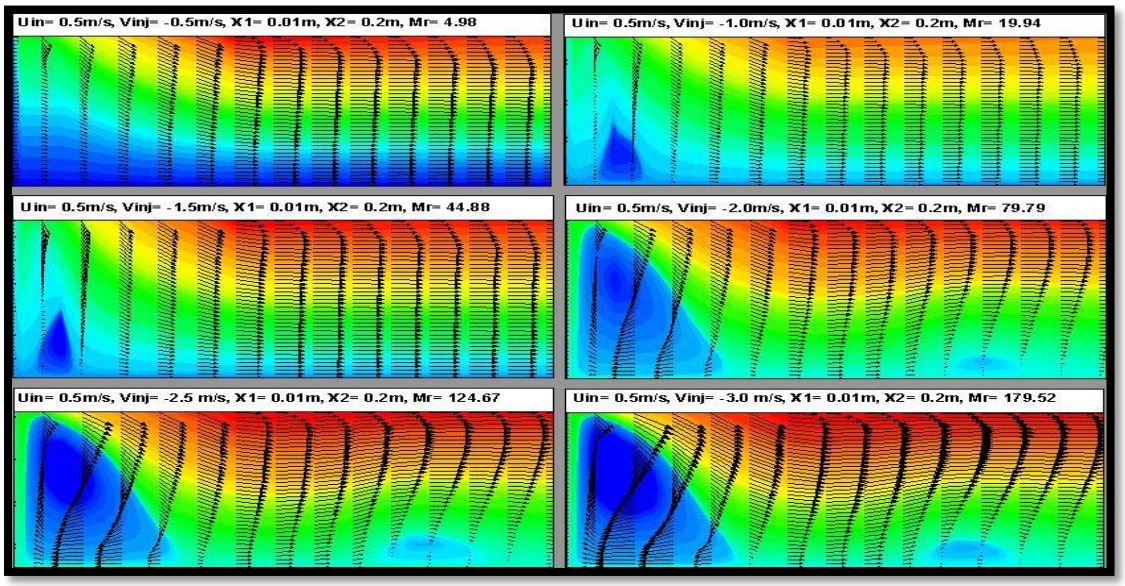

Figure 5, Effects of side injection velocity on the main flow.

3.4 Effects of the Axial Extent of Side Injection on the Main Flow

The Effect of side injection on the main turbulent fluid flow due to the variation of the axial extent of side injection keeping other parameters constant has been shown in fig. 6. The inlet fluid velocity and side injection velocity has been taken as 0.5 m/s and -2 m/s respectively and the axial extent has been varied from 0.19 m to 0.99 m. As the axial extent of side injection has been increased, the mass of side injected fluid also increases. In other words there is an enhancement of the penetration depth, mixing phenomena causing increased NOx accumulation and local temperature rise etc due to increase in side injection width. These findings are in accordance of the discussions as already has been done.

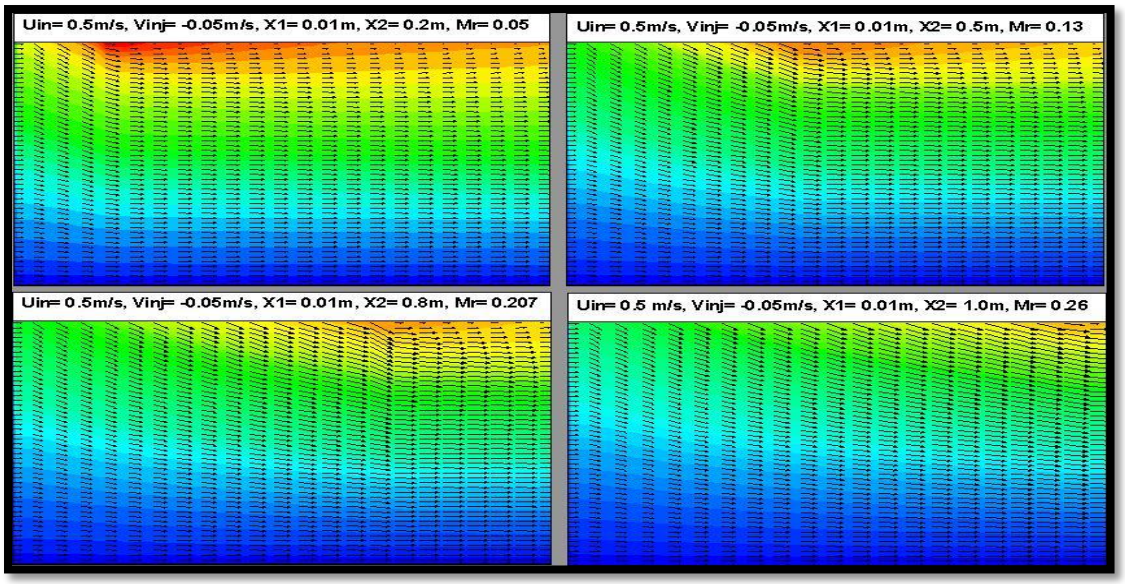

Figure 6, Effects of the axial extent of side injection on the main flow.

3.5 Effects of Axial Position of the Side Injection Zone

The axial position of the onset of side mass injection plays a vital role on the onset and size of the recirculation formed in the main turbulent flow. In fig. 7, the location of the side injection site has been changed towards the downward direction with inlet uniform axial velocity U_{in} = 0.5 m/s and side injection velocity, V_{inj} =-0.1 m/s. In the first plot the side injection site has been placed at a distance of 10% of the length of the duct and gradually the distance of the injection site from the inlet has been increased and the site has been placed at a distance of 25%, 50% and 75% of the length of the duct. The extent of the injection site has been kept constant as 0.1 m. This signifies that as the side injection site has been relocated by changing its position towards downstream, the penetration due to the injection in the flow at the inlet become less effective, because under such condition the majority of the duct flow at upstream does not come across under the purview of the side injection. This is because there will be less confrontation between the inlet flow and side injected flow and will be no adverse pressure gradient at the upstream side of the bulk flow. So, it is possible to get a uniform flow at inlet in a cylindrical duct even by using the side injection mass if it is placed beyond certain axial position of the cylinder. Such a condition is sometimes very much worthy in the sense that less NOx and local heating is possible with all of the benefit of the side injection of mass in a main turbulent flow.

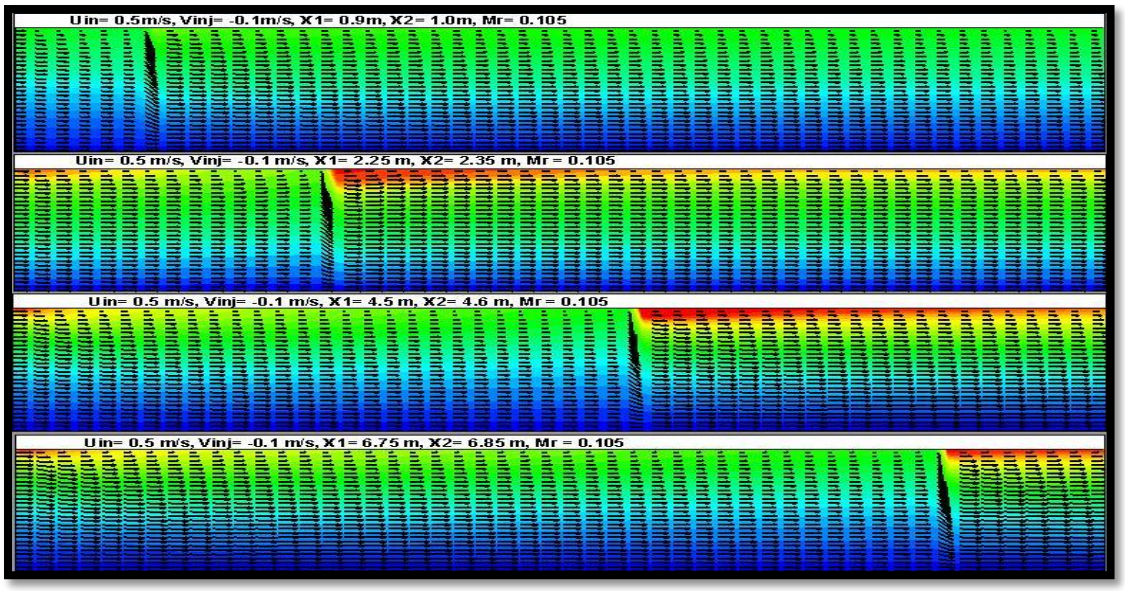

Figure 7, Effects of axial position of the onset of the side injection zone.

In the fig. 8, the non-dimensional penetration depth variation with respect to momentum ratio of the injection velocity to the inlet main velocity has been presented. From the figure, it is observed that the penetration depth is dependent on this momentum ratio. The penetration depth gradually increases in a non-linear fashion when the momentum ratio of injection velocity and inlet mean velocity increases. This is very much compatible with the physical condition of the flow.

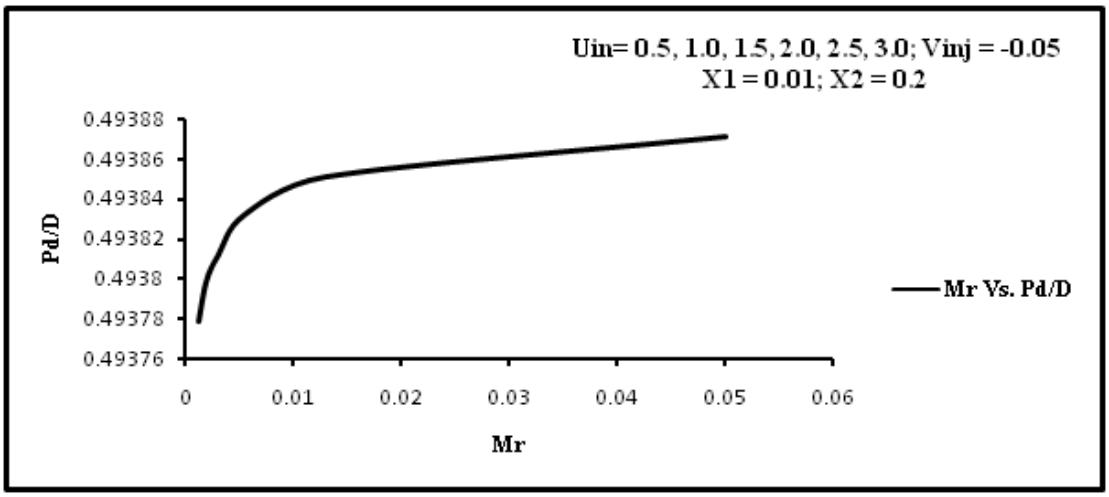

Figure 8, Non-dimensional Penetration Depth vs. Non-dimensional Injection velocity

In the fig. 9 and 10, we observe the variation of the recirculation depth (fig. 9) and width (fig. 10) with the momentum ratio of injection velocity to the mean inlet velocity the figures we can observe that both the recirculation depth and recirculation

width increase gradually with this ratio.

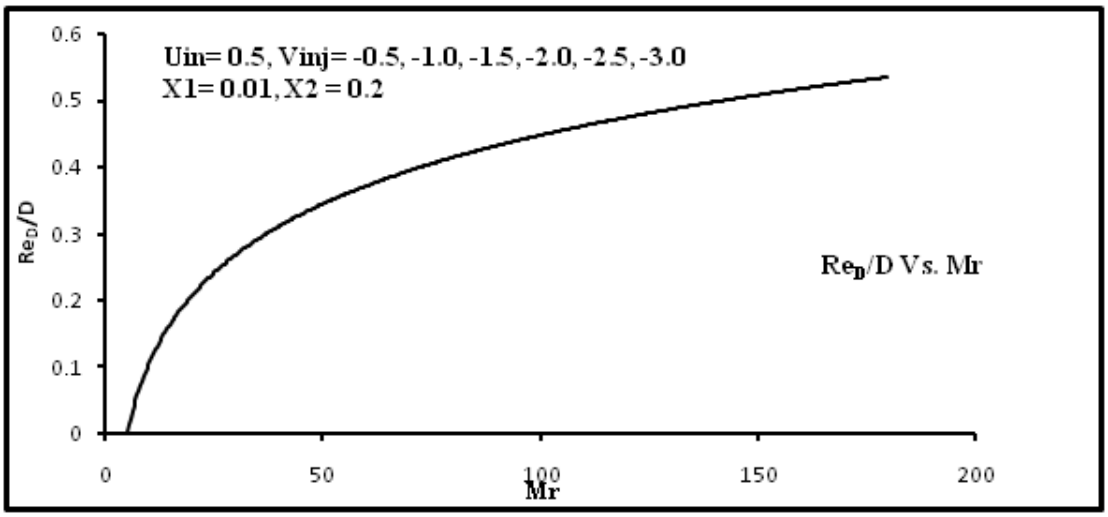

Figure 9, Non-dimensional Recirculation Depth vs. Non-dimensional Injection Velocity

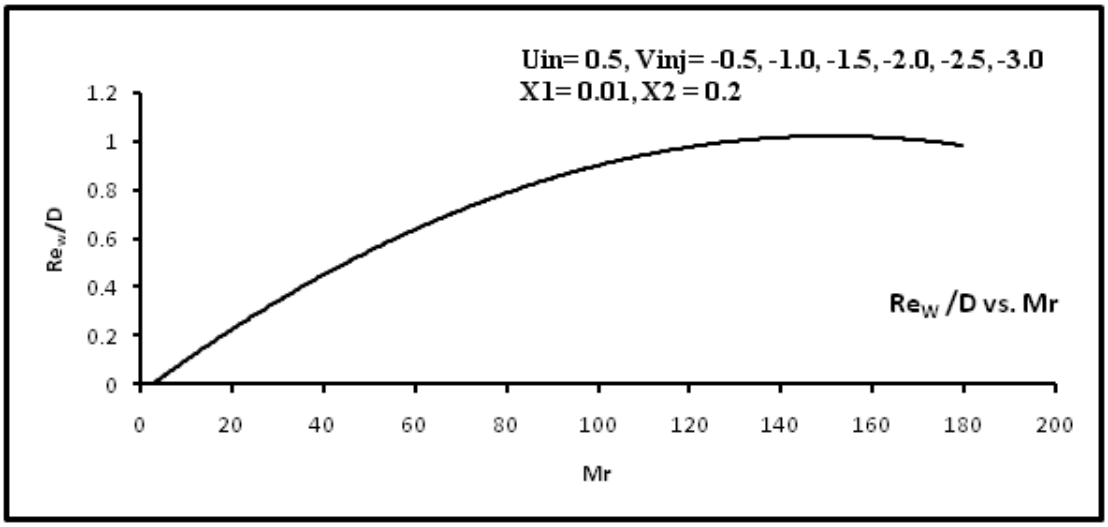

Figure 10, Non-dimensional Recirculation Width vs. Non-dimensional Side injection Velocity.

4 Conclusions

The turbulent fluid flow through an axi-symmetric circular duct with side mass injection has been thoroughly investigated. The side mass injection plays an important role on flow pattern of the main turbulent flow in the circular duct. The principle conclusions from the numerical analysis summarized herein are:

1. The penetration depth of the side injection is dependent on the momentum ratio of injection velocity to the mean inlet velocity (Mr) and it decreases with the decrement of this ratio.

2. The variation of the side injection velocity changes the flow pattern of the main flow significantly. With the increase of the side injection velocity the penetration depth increases and a recirculatory flow of reasonable strength generated. The size of width and depth of recirculation bubble increases as Mr increases. However, the recirculatory flow does not appear if this momentum ratio is less than 5.0.
3. The effect of side injection increases with the increase of the axial extent of side injection. A large mass of main turbulent flow comes under the purview of penetration with a bigger extent of side injection.

Nomenclature:

C_μ	Empirical constant
C_t	Craya- Curtet number
D	Diameter of the cylindrical duct, m
f	Friction factor
G	Production term
K_1, K_2	Constants
L	Length of the cylindrical duct, m
Mr	Momentum ratio of side mass flow to the main axial flow
$\vec{n}$	Unit normal vector
Pd	Penetration Depth, m
R	Radius of the cylindrical duct, m
r	Radial co-ordinate across the duct
R_W	Recirculation Width, m
R_D	Recirculation Depth, m
R_c	Radius of curvature of the streamline
$\vec{s}$	Unit tangential vector
$\bar{u}$	Time mean velocity along x-axis, m/s
U_{in}	Inlet flow velocity, m/s
U_{mean}	Mass-averaged mean axial velocity, m/s
$\bar{v}$	Time mean velocity along y-axis, m/s
V_{inj}	Side injection velocity, m/s
X	Axial co-ordinate along the duct, m
Re	Reynolds Number = $\frac{\rho v D}{\mu}$

Greek Letters

ε	Turbulent dissipation rate, m^2/s^3
k	Turbulent kinetic energy, m^2/s^2
μ	Viscosity of the air, kg/m-s
μ_{eff}	Effective viscosity, kg/m-s
μ_l	Laminar viscosity, kg/m-s
μ_t	Eddy viscosity, kg/m-s
ψ	Stream function, m^2/s
ρ	Density of air, kg/m^3

Acknowledgements:

The work is supported by Council of Scientific and Industrial Research (CSIR) of Govt. of India.

References:

[1] [1] Laufer, J., 1954, "The Structure of Turbulence in Fully Developed Pipe Flow", NACA report no. 1174.

[2] [2] Barchilon, M. and Curet, R., 1964, "Some Details of the Structure of an Axi-Symmetric Confined Jet With Backflow", Trans. ASME, J. Basic Engg. 86, pp. 777-786.

[3] [3] Olson, R. M. and Eckert, E. R. G., 1966, "Experimental Studies of Turbulent Flow in a Porous Circular Tube with Uniform Fluid Injection through the Tube Wall", J. Appl. Mech. March, pp. 7-17.

[4] [4] Ei-Nashar, A. M., 1974, "Turbulent Flow in an Annulus with Injection. An Experimental Study", Ind. Eng. Chem. Fundam. 13, pp. 33-38.

[5] [5] Launder, B. E. and Spalding, D. B., 1974, "The Numerical Computation of Turbulent Flows", Comput. Methods in Appl. Mech. 3, pp. 269-289.

[6] [6] Patankar, S.V., 1981, "Numerical Heat Transfer and Fluid Flow", McGraw-Hill, New York.

[7] [7] Leschziner M. A. and Rodi, W., 1981, "Calculation of Annular and Twin Parallel Jets Using Various Discretization Schemes and Turbulence-Model Variations", Trans. ASME, J. Fluids Engg. 103, pp. 352-360.

[8] [8] Chang, Y. R. and Chen, K. S., 1995, "Prediction of Opposing Turbulent Line Jets Discharged Laterally into a Confined Cross Flow", International J. Heat and Mass Transfer. 38, pp. 1693-1703.

[9] [9] Tong-Miin, L., Chin-Chun, L., Shih-Hui, C., and Hsin-Ming, L., 1999, "Study on Side-Jet Injection Near a Duct Entry with Various Injection Angles", J. Fluid Engg.. 121, pp. 580-587.

[10] [10] Hold, A. E., Calay, R. K. and O'Brien, M., 2002, "Flows Generated by the Interaction of an Inlet and a Cross Flow", J. Wind Engineering And industrial Aerodynamics. 88, pp.1-23.

[11] [11] Tao, Y., Adler, W. and Specht, E., 2002, "Numerical Analysis of Multiple Jets discharging into a confined cylindrical cross flow", J. Process Mechanical Engg. 216, pp.173-180.

[12] [12] Kelman, J. B., Greenhalgh, D. A. and Whiteman, M., 2006, "Micro Jets in a Confined Turbulent Cross Flow", J. Experimental Thermal and Fluid Science. 30, pp. 297-305.

[13] [13] Ko, T. H., 2006, "A Numerical Study on the Effects of Side Inlet Angle on the Mixing Phenomena in a Three Dimensional Side Dump Combustor", International Communications in heat and mass transfer. 33, pp. 853-862.

[14] [14] Ting-ting, G. and Shao-hua, L., 2006, "Numerical Simulation of Turbulent Jets with Lateral Injection into a Cross Flow", Journal of Hydrodynamics. 18, pp. 319- 323.

[15] [15] Majumder, S. and Sanyal, D., 2008, "Destabilization of Laminar Wall Jet Flow and Re-Laminarization of the Turbulent Confined Jet Flow in Axially Rotating Circular Pipe", Trans. ASME, Journal of Fluids Engg. 130, pp. 011203-1 – 011203-8.

[16] [16] Guo, H. F., Chen, Z. Y. and Yu, C. W., 2009, "Simulation of the Effect of Geometric Parameters on Tangentially Injected Swirling Pipe Flow", Comput. & Fluids. 38 , pp. 1917-1924.

[17] [17] Kollmann, W. and Umont, G., 2009, "Formation of a recirculation zone in low Re-number turbulence", Comput. & Fluids. 38, pp. 1424-1434.